

# Medical imaging using capacitive micromachined ultrasonic transducer arrays

Jeremy Johnson<sup>a,b,\*</sup>, Ömer Oralkan<sup>a</sup>, Utkan Demirci<sup>a</sup>, Sanlı Ergun<sup>a</sup>,  
Mustafa Karaman<sup>a</sup>, Pierre Khuri-Yakub<sup>a</sup>

<sup>a</sup> Edward L. Ginzton Laboratory, Stanford University, 450 Via Palou, Stanford, CA 94305, USA

<sup>b</sup> Image Guidance Laboratories, Stanford University, Stanford, CA 94305, USA

## Abstract

We are investigating the use of capacitive micromachined ultrasonic transducers (cMUT's) for use in medical imaging. We propose an ultrasound probe architecture designed to provide volumetric ultrasound imaging from within an endoscope channel. A complete automated experimental system has been implemented for testing the imaging performance of cMUT arrays. This PC-based system includes custom-designed circuit boards, a software interface, and resolution test phantoms. We have already fabricated 1D and 2D cMUT arrays, and tested the pulse-echo imaging characteristics of 1D arrays. Beamforming and image formation algorithms that aim to reduce the complexity of data acquisition hardware are tested via numerical simulations and using real data acquired from our system. © 2002 Elsevier Science B.V. All rights reserved.

*Keywords:* Capacitive micromachined ultrasonic transducer; Medical imaging; Three-dimensional ultrasound; Two-dimensional ultrasound array

## 1. Introduction

Real-time volumetric imaging using 2D transducer arrays is an important topic of current medical imaging research. The potential impact of volumetric imaging is enormous; volumetric imaging has the potential to extend the frontiers of traditional diagnostic ultrasound by providing a complete visualization of internal tissue along with 3D flow information, thus challenging other off-line 3D imaging methods. Moreover, volumetric scanning has the potential to make ultrasound imaging a unique real-time guidance tool for surgical and therapeutic operations. These characteristics are unmatched by current surgical guidance imaging modalities, which either require off-line processing, have harmful biological side effects, or provide only 2D images.

Volumetric ultrasound scanners that use 2D arrays contain hundreds of elements, and hence require excessive numbers of parallel front-end processing channels.

Realization of the front-end hardware is a major difficulty in designing volumetric systems. Combining this with the difficulties of 2D transducer design, full-scale real-time volumetric imaging has not yet succeeded. However, various volumetric imaging studies based on sparse array processing [1], parallel beamforming [2], and 3D image registration [3,4] have been reported in the literature. Sparse array processing reduces the front-end complexity, but at the expense of significant degradation in image quality. Parallel transmit and receive beamforming is used to reduce the firing events to improve the frame rate. 3D image registration involves off-line or pseudo-real-time reconstruction using successive 2D image frames and measuring and/or extracting the probe motion.

We propose an ultrasound probe architecture for volumetric imaging designed for use during minimally invasive surgical procedures where real-time imaging and small probe size are of primary concern. The proposed architecture involves a small number of front-end processing channels with multiplexed active subarrays on a large transducer array. The analog front-end circuitry and digital-to-analog conversion circuitry will be part of the ultrasound probe. Since space is limited, and

\* Corresponding author. Tel.: +650-723-0697/533-5533; fax: +650-725-2533.

E-mail address: jeremyj@stanford.edu (J. Johnson).

because we wish to minimize the complexity of the front-end hardware, it is desired to keep the number of parallel processing channels to a minimum. This receive channel limitation is the first motivation to investigate new methods of beamforming and image formation. We propose using a synthetic aperture method of beamforming which requires only using a small fraction of the total number of array elements at any given time. An equivalent 1D version of this method is described in [5].

We use capacitive micromachined ultrasonic transducers (cMUT) since they provide large bandwidth, good sensitivity, and a potential for electronic integration [6,7]. We have successfully constructed cMUT arrays with 100% fractional bandwidth, twice that of piezoelectric transducers. With this improved bandwidth of cMUT arrays, higher spatial resolution is achieved. In addition, it presents a second motivation for investigating new beamforming and image reconstruction algorithms that do not rely on narrow bandwidth.

An experimental ultrasound system has been constructed for achieving three goals: (1) implement a large-scale approximation of our proposed probe architecture, (2) characterize cMUT arrays, and (3) collect real data on which to perform new beamforming and image reconstruction algorithms.

## 2. Ultrasound probe architecture

The architecture of the volumetric scanning probe is shown in Fig. 1. The beam lines sweep out a solid angle of  $90^\circ$  and reasonable lateral and longitudinal resolutions extend to a depth of 5 cm. The system is designed to operate at a center frequency of 5 MHz. For a  $16 \times 16$  2D array with square elements measuring  $150 \mu\text{m}$  per side, the total array measures 2.4 mm on each side. The physical dimensions of the array make it suitable for use within an endoscopic channel during minimally invasive surgery. The system will acquire volumetric images up to 15 frames per second.

A key feature of the design is that the 2D cMUT wafer is flip-chip bonded to a separate die with front-end processing circuitry. Each array element contains a through-wafer via that is connected to the processing circuitry. In order to reduce the number of front-end parallel processing channels for transmit and receive, and to maintain real-time imaging, we employ our novel subarray-processing algorithm. Rather than firing and receiving on all 256 channels to acquire data for each beam line, A-scans are acquired using only one  $4 \times 4$  subarray for transmit and another subarray for receive for a given firing event. The result is that only 16 transmit and 16 receive channels are necessary. A multiplexer (MUX) selects the active transmit and receive subarrays.

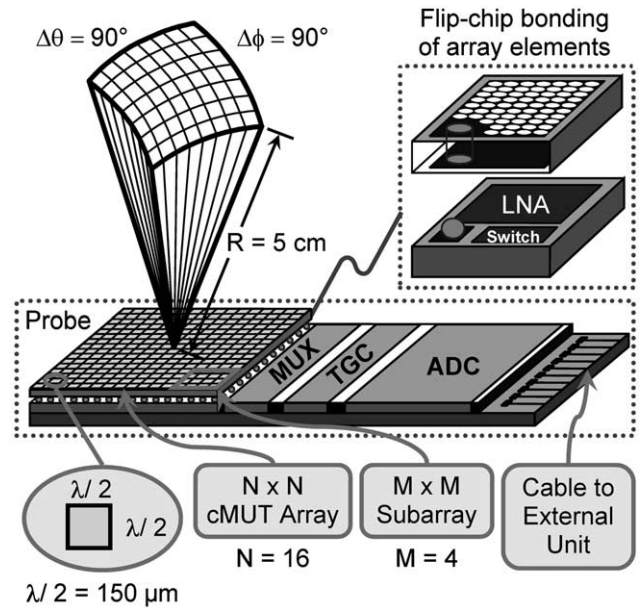


Fig. 1. Diagram of probe architecture and scanning volume. The imaging volume is pyramidal in shape, extends to a depth of 5 cm and scans a sector of  $90^\circ$ . Element size is chosen to meet the Nyquist sampling criteria in beamspace. The cMUT array is flip-chip bonded to front-end processing electronics, which include a MUX for selecting transmit and receive subarrays, amplifiers for TGC, and ADCs. The number of parallel receive channels are reduced by using subarray processing.

The probe electronics contain both the analog front-end (AFE) circuitry as well as analog-to-digital converters (ADC) for digitizing the received signals prior to transmitting them to the external processing unit for image reconstruction and visualization. The AFE contains the MUXs, pre-amplifiers, variable-gain amplifiers for time-gain compensation (TGC), and anti-alias filters. A custom-designed ADC has a pipeline architecture to digitize all 16 signals simultaneously.

A significant advantage of digitizing the received echo signals within the probe itself is that the signals can be transmitted without loss to the ultrasound base unit. The high-speed digital communication link between the probe and the base can be made with a single shielded cable between the two. This method eliminates the current need for a large number of shielded coaxial wires bundled into an excessively large cable.

## 3. cMUT arrays

Unlike piezoelectric transducer elements, which are formed from a solid material with electrodes on opposite sides, cMUT transducers consist of a sealed cavity beneath a membrane (Fig. 2). Electrodes lie at the base of the cMUT cell as well as above the membrane. The force between the plates of this “capacitor” causes the membrane to vibrate and emit acoustic energy upon the ap-

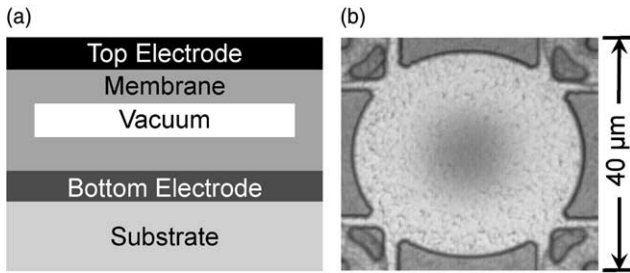


Fig. 2. A cMUT cell. (a) A cross-sectional model of a cMUT cell and (b) a photograph of the top of a cMUT cell.

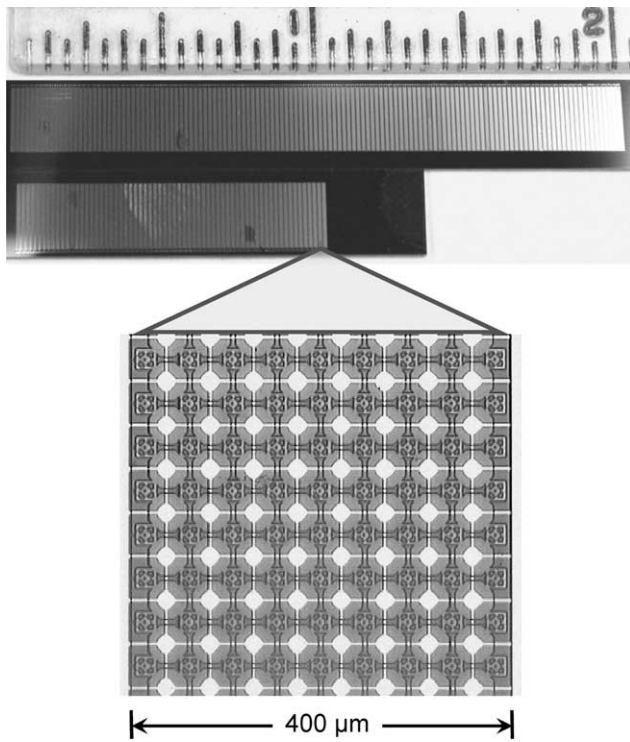


Fig. 3. 1D cMUT arrays. Top: 128- and 64-element cMUT arrays. Bottom: portion of a single cMUT element containing hundreds of cMUT cells.

plication of an electrical pulse. A single array element is made up of tens or hundreds of cMUT cells acting in parallel.

We have experience fabricating both 1D and 2D cMUT arrays. Fig. 3 shows a 64- and 128-element 1D array with a close-up of a portion of a single array element showing individual cMUT cells. Electrical connections to the 1D arrays are made by wire bonding to pads located near the end of each element. A  $128 \times 128$ -element 2D array is shown in Fig. 4 along with a close-up of an array element. The close-up shows the through-hole via that is used to provide electrical connectivity from the backside of the wafer. A  $16 \times 16$  subsection of this array is currently being flip-chip bonded to a fan-

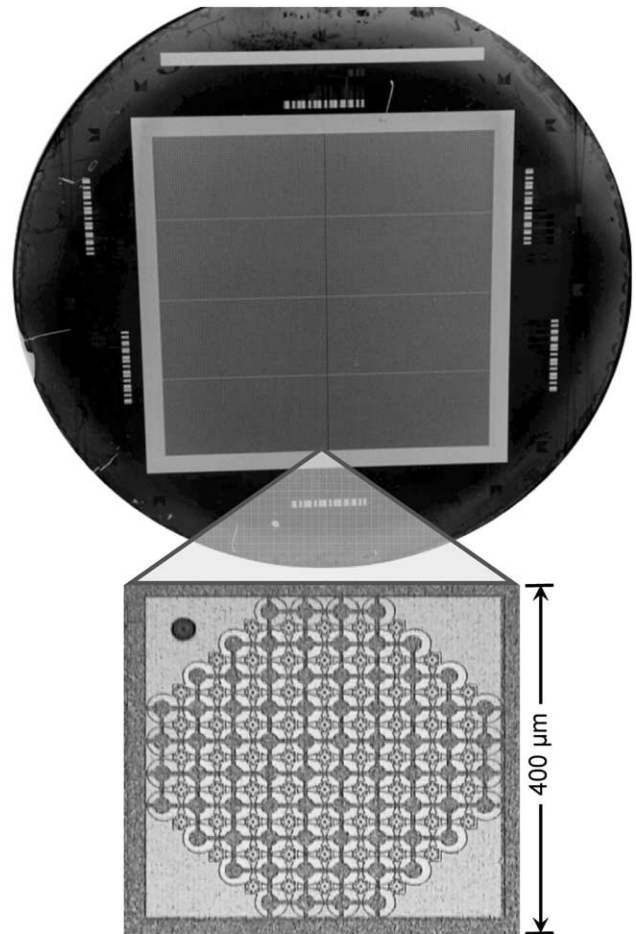


Fig. 4. 2D cMUT array. Top:  $128 \times 128$ -element 2D cMUT array composed of 8 adjacent  $64 \times 32$  arrays manufactured on a 4" diameter wafer. Bottom: a single cMUT element containing 76 cMUT cells. The through-wafer via shown in the top-left corner provides an electrical connection to the element from the backside of the wafer.

out substrate that will provide pads for wire bonding around the edges of the array.

#### 4. Numerical simulations

We have investigated the use of different beamforming algorithms to reduce the complexity of the front-end circuitry. In addition to testing the algorithms on real data, we evaluate them using numerical calculations of the point-spread function (PSF). For example, Fig. 5 compares the differences in the PSFs of a multi-element synthetic aperture algorithm to traditional full phased array processing. Unlike full phased array processing, which transmits and receives on all elements to form each beam line, multi-element synthetic aperture processing only transmits and receives on a small subset of adjacent elements, reducing the number of front-end processing channels. The combined response of the subarrays achieves full-aperture resolution.

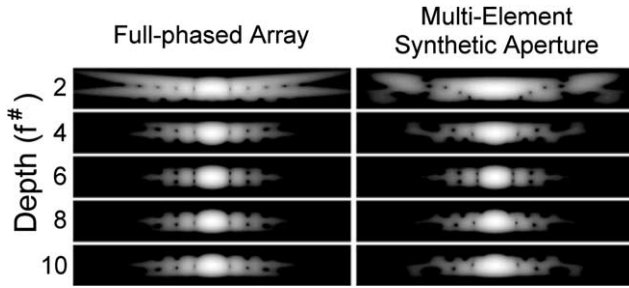


Fig. 5. Numerical simulations of a 16-element 1D array PSF using two different beamforming methods. Left: full-phased array beamforming; Right: multi-element synthetic aperture beamforming using only one 4-element subarray per firing event. All images displayed on a 40 dB log scale.

**5. cMUT imaging characteristics**

The experimental system has been used to characterize the cMUT’s as imaging devices. A typical A-scan of a wire phantom submerged in oil is shown in Fig. 6a. The frequency response of the received signal is shown in Fig. 6b. Although this response is a function of the transmitted signal, media characteristics, and transducer properties, it shows the wide bandwidth property of cMUT’s. The simulated and experimental PSFs are compared in Fig. 6c.

Preliminary imaging results are shown in Fig. 7. The image was formed from individual A-scans of a wire phantom. A 16-element 1D cMUT array was used with full phased array beamforming with dynamic transmit and receive focusing. The image shows that very good axial resolution is produced by the cMUT array with wide temporal bandwidth. The low lateral resolution, however, is due to the small size of the imaging array ( $N = 16$ ).

**6. Experimental system**

In order to test the imaging capabilities of cMUT arrays and to evaluate novel beamforming and image reconstruction algorithms on real ultrasound data, an experimental system (Fig. 8) has been built to automatically collect A-scan data from cMUT arrays with up to 64 elements. The design of the system parallels the probe architecture mentioned earlier, and provides us with a platform for testing as we work to miniaturize the electronics.

The imaging tank is made of acrylic, is roughly 0.3 m tall with a 0.5 m square footprint, and is filled with water. Inside sits an acrylic frame that holds a series of 200  $\mu\text{m}$  stainless steel wires under tension. The wires are evenly spaced, parallel, and form a plane perpendicular to the ultrasound-imaging plane.

A fan-out circuit board (Fig. 9c) provides electrical connections between the array elements and the front-

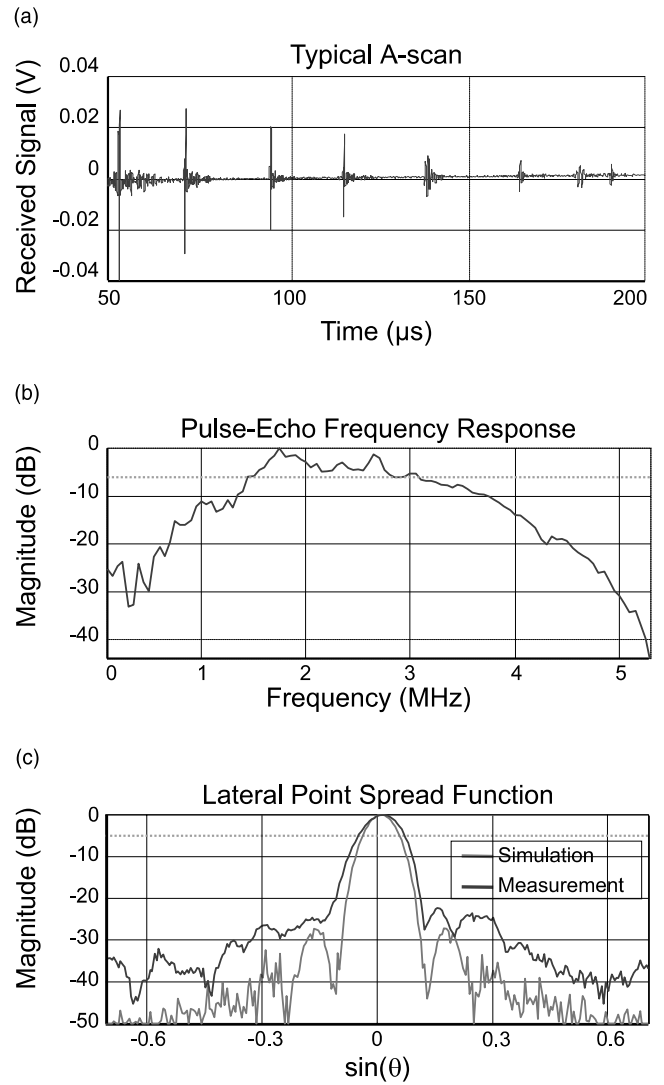


Fig. 6. cMUT imaging characteristics. (a) Typical received pulse-echo signal of a multi-wire phantom, (b) the Fourier transform of the received time signal demonstrating the wide bandwidth characteristic of cMUT’s, (c) simulated and experimental PSF.

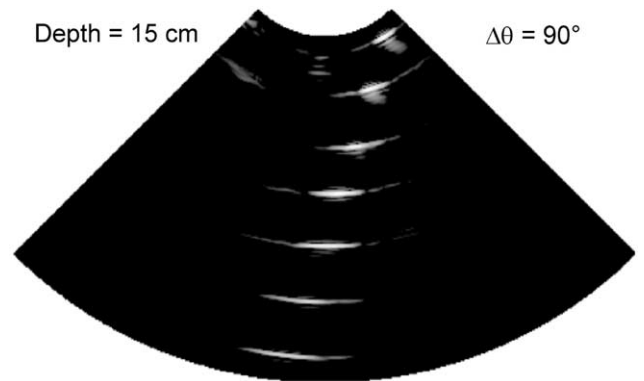


Fig. 7. 2D image using a 16-element cMUT array, reconstructed by using full-phased array beamforming on pulse-echo data.

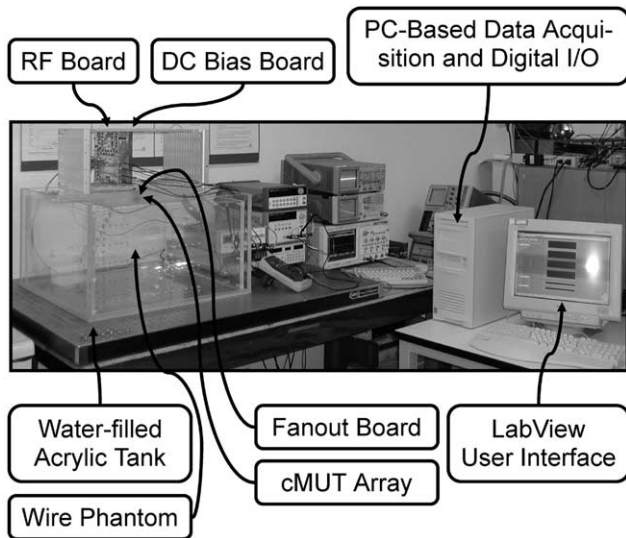


Fig. 8. Experimental system. The system is used for characterization of the cMUT arrays as well as data acquisition for algorithm testing. The system automatically collects pulse-echo data at from up to 64-element arrays and stores the data for offline beamforming. An off-the-shelf PC-based data acquisition board digitizes four channels at 20 MHz and with 12-bit resolution.

end circuitry. The cMUT array is firmly attached to the fan-out board and wire bonded to the circuit board.

A short coaxial ribbon cable connects the fan-out board to the DC bias board. The DC bias board (Fig. 9b) applies a high DC voltage to each cMUT element that is necessary for operation. Another ribbon cable connects the DC bias board to the RF board.

The RF board (Fig. 9a) provides transmit and receive channel selection and amplification of the incoming echo signals. Video MUXs are used to enable any number of channels for transmit, and up to four channels for receive. Typically the system is used for collecting A-scans from all transmit/receive channel combinations, in which case only one transmit channel is selected at a time. The switches have a serial I/O interface that allows remote channel selection and feedback of the most recently activated elements. Variable-gain amplifiers amplify the four received channels such that their voltage range is suitable for digitization.

The four channels are then input to an off-the-shelf digital-to-analog converter PCI card (Measurement Computing DAS4020-12). The card simultaneously digitizes the incoming signals at 20 MHz with 12-bit resolution. The digital I/O interface is used to control the serial I/O lines of the MUXs.

Finally, custom-designed data acquisition software controls the data acquisition (Fig. 10). The acquisition tool displays the incoming waveforms as they are captured and shows the active transmit and receive channels. A-scans from all transmitter/receiver combinations can be automatically acquired and stored to disk. The

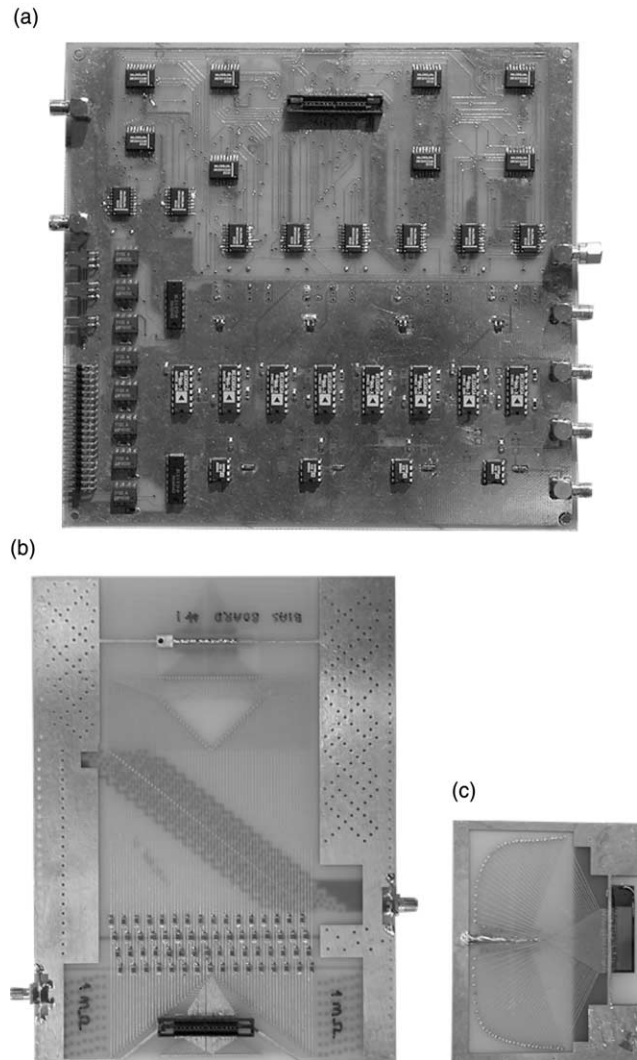


Fig. 9. Custom-designed circuit boards used in the experimental system. (a) The RF board uses video MUXs to select any of the 64 elements for transmit, and up to four elements for receive. The MUXs are set via a serial I/O channel. Variable gain amplifiers adjust the received echo signals to the appropriate voltage range for digitization, (b) the DC bias board applies the bias to all cMUT elements that is necessary for operation, (c) the cMUT array is fixed to and the elements are wire-bonded to the fan-out board, which provides electrical connection to the DC bias board and the RF board.

stored A-scans are used to test beamforming algorithms offline.

## 7. Conclusion

The characteristics of cMUT arrays make them viable candidates for 2D ultrasound arrays for real-time volumetric imaging. The significant improvements in bandwidth and sensitivity as compared with piezoelectric transducers provide an opportunity for exploring new beamforming algorithms to achieve enhanced image

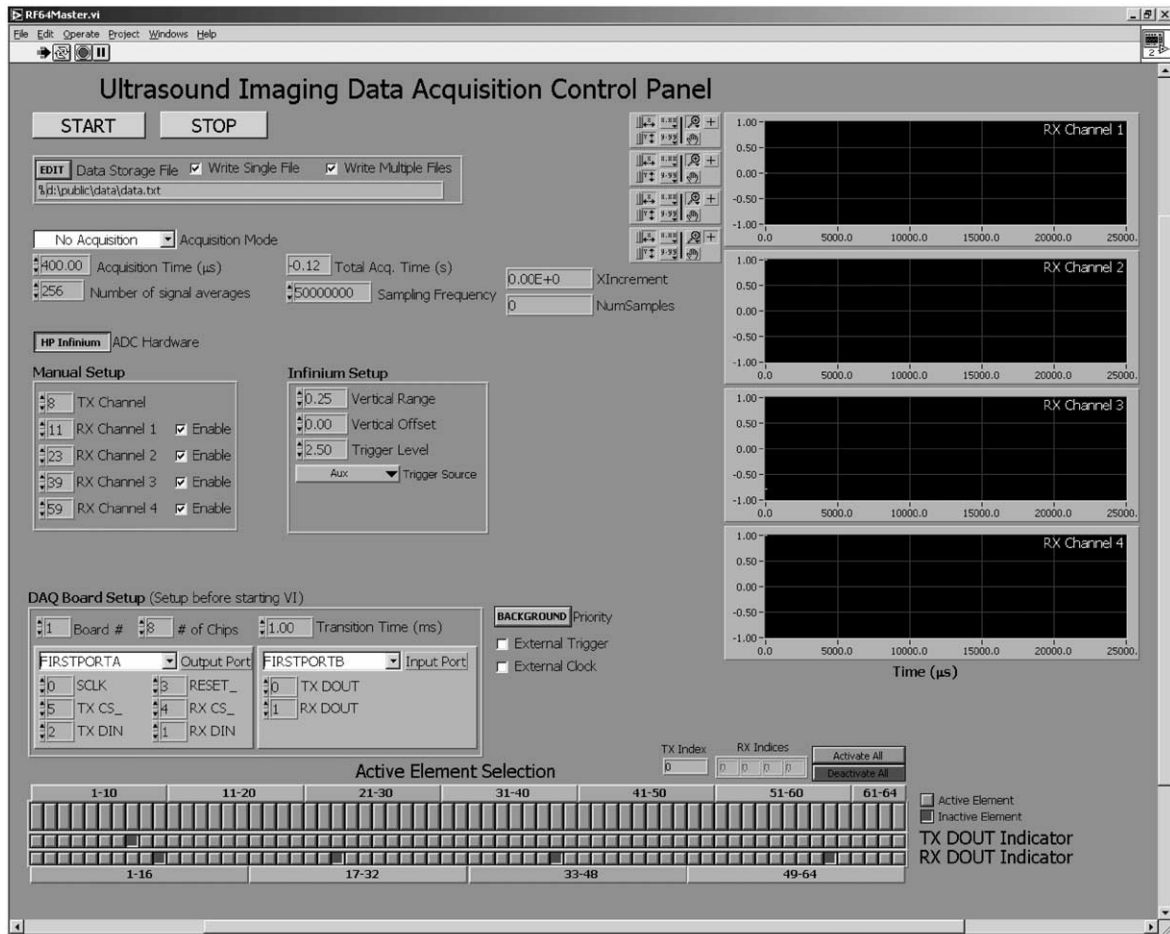


Fig. 10. Acquisition software. The custom-designed user interface and supporting software automates the data collection procedure. A-scan data from all transmit/receive element combinations can be acquired and stored automatically. Received signals on the four A/D channels are displayed in separate graphs. The current transmit channel and receive channels are indicated in a graphical display at the bottom.

quality. The use of subarray processing allows real-time imaging and reduces the number of front-end processing channels so that the front-end integrated to the array can be mounted into a miniature probe. The proposed probe architecture with a  $16 \times 16$  cMUT array will fit inside of a 5 mm endoscopic channel, providing surgeons with real-time 3D ultrasound during endoscopic and laparoscopic surgery.

## References

- [1] G.R. Lockwood, F.S. Foster, Optimising the radiation pattern of sparse periodic two-dimensional arrays, *IEEE Trans. Ultrason. Ferroelect. Freq. Contr.* (January) 43 (1996) 15–19.
- [2] S.W. Smith, H. Puly, O.T. von Ramm, High-speed ultrasound volumetric imaging systems: Part I: transducer design and beam steering, *IEEE Trans. Ultrason. Ferroelect. Freq. Contr.* (March) 38 (1991) 100–108.
- [3] R. Shahidi, R. Tombropoulos, R. Grzeszczuk, Clinical applications of three-dimensional rendering of medical data-sets, *Proc. IEEE* 86 (3) (1998).
- [4] J. Nerney Welch, J.A. Johnson, M.R. Bax, R. Badr, R. Shahidi, A real-time freehand 3D ultrasound system for image-guided surgery, *IEEE Ultrason. Symp.* (2000).
- [5] M. Karaman, M. O'Donnell, Subaperture processing for ultrasonic imaging, *IEEE Trans. Ultrason. Ferroelect. Freq. Contr.* (January) 45 (1) (1998) 126–135.
- [6] Ö. Oralkan, X. Jin, K. Kaviani, A. Ergun, F. Degertekin, M. Karaman, B. Khuri-Yakub, Initial pulse-echo imaging results with one-dimensional capacitive micromachined ultrasonic transducer arrays, *IEEE Ultrason. Symp.* (2000).
- [7] Ö. Oralkan, X. Jin, F. Degertekin, B. Khuri-Yakub, Simulation and experimental characterization of a 2D capacitive micromachined ultrasonic transducer array element, *IEEE Trans. UFFC* 46 (1999) 1337–1340.